

RobWE: Robust Watermark Embedding for Personalized Federated Learning Model Ownership Protection

Yang Xu¹, Yunlin Tan¹, Cheng Zhang¹, Kai Chi¹, Peng Sun¹, Wenyuan Yang²,
Ju Ren³, Hongbo Jiang¹, Yaxue Zhang³

¹Hunan University, ²Sun Yat-sen University, ³Tsinghua University

Abstract

Embedding watermarks into models has been widely used to protect model ownership in federated learning (FL). However, existing methods are inadequate for protecting the ownership of personalized models acquired by clients in personalized FL (PFL). This is due to the aggregation of the global model in PFL, resulting in conflicts over clients' private watermarks. Moreover, malicious clients may tamper with embedded watermarks to facilitate model leakage and evade accountability. This paper presents a robust watermark embedding scheme, named RobWE, to protect the ownership of personalized models in PFL. We first decouple the watermark embedding of personalized models into two parts: head layer embedding and representation layer embedding. The head layer belongs to clients' private part without participating in model aggregation, while the representation layer is the shared part for aggregation. For representation layer embedding, we employ a watermark slice embedding operation, which avoids watermark embedding conflicts. Furthermore, we design a malicious watermark detection scheme enabling the server to verify the correctness of watermarks before aggregating local models. We conduct an exhaustive experimental evaluation of RobWE. The results demonstrate that RobWE significantly outperforms the state-of-the-art watermark embedding schemes in FL in terms of fidelity, reliability, and robustness.

1. Introduction

Training artificial intelligence models demands substantial resources, and thus well-trained commercial models have evolved into pivotal assets for many corporations [12, 13, 41]. Unfortunately, models are confronted by pronounced risks of intellectual property infringement. Previous studies have unveiled that models may be illicitly leaked during usage or even stolen through model imitation attacks [14, 29, 31, 39]. Therefore, guaranteeing ownership of models has become an urgent imperative.

Model watermarking is an effective technology for model ownership confirmation. Specifically, model watermarking involves embedding identifiable or distinctive markers into models based on features or backdoors. The model owner can proof the ownership by extracting the watermark in the model when the ownership dispute occurs. Initial model watermarking studies primarily focused on guaranteeing ownership in traditional machine learning scenarios. Recently, with the rise of federated learning (FL), there has been a considerable surge of interest in protecting model ownership within distributed machine learning scenarios. FL, as a privacy-preserving machine learning, facilitates collaborative training of models without collecting client data [24]. However, as each client in FL has access to the trained models, FL is susceptible to heightened risks of model leakage. Besides, the distributed model training process of FL also poses challenges for watermark embedding and identification.

To protect the intellectual property of models in FL, federated model ownership verification schemes have been proposed. Waffle [30] is the pioneering effort. It proposed to embed watermarks when the server aggregates local models to protect global model ownership. Considering client contributions within FL, subsequent approaches [17, 22] permit clients to embed private watermarks during local model training, facilitating independent verification of model ownership by all parties. However, these schemes confine to the vanilla FL paradigm, rendering them susceptible to performance degradation in real-world scenarios where the data among clients is non-independent and identically distributed (non-IID).

To account for such data heterogeneity, researchers have proposed the framework of personalized federated learning (PFL), such as clustered FL [6, 10, 26] and federated meta learning [3, 7]. PFL not only leverages the collective knowledge from the distributed data sources to train a shared global model but also allow client to tailor personalized models according to their specific data distributions. Unfortunately, while it allows for more tailored and effective models for clients with heterogeneous data distributions

or unique preferences, PFL faces the following three-fold challenges in preserving the ownership of these personalized models:

- First, personalized model ownership currently has no corresponding solution. Existing solutions focus on embed client watermarks within the shared global model in FL. If PFL adopts these schemes directly, after aggregation, personalized models will encompass watermarks from other clients, failing to satisfy the private nature of personalized model ownership.
- Second, the model obtained by PFL also contains all clients’ knowledge contributions. To declare the contributions of all clients, embedding a public watermark into the model is a natural idea. However, watermarks from different clients conflict in the same embedding region. While some preliminary solutions exist, their efficacy is insufficient when the number of participants is large and the watermark bits is long [17, 22, 35].
- Third, some malicious clients do not comply with the watermark embedding protocol. Instead, they may insert falsified watermarks, making it challenging to verify model ownership when disputes happen.

Motivated by the above discussions, this paper presents a robust watermark embedding scheme, named RobWE, to protect the ownership of personalized models in PFL. RobWE disentangles the watermark embedding process into two distinct components tailored for personalized FL scenarios: head layer embedding and representation layer embedding. The head layer, constituting the client’s private segment, remains separate from model aggregation, while the representation layer is part of the client’s shared segment. Hence, the watermark slice within the representation layer signifies the client’s contribution to the global model, while the private watermark within the head layer elucidates ownership of the personalized model. Furthermore, we employ a watermark slice embedding operation within the representation layer to mitigate conflicts arising from model aggregation and the embedding of multiple watermarks. This operation also prevents malicious clients from tampering with the unique watermark to evade detection. Finally, we propose a tampered watermark detecting mechanism to thwart adversaries, which enables the server to validate the accuracy of client watermark slices before aggregating corresponding representation models. Specifically, the server extracts the client watermark slice from the representation model and determines whether it is honestly embedded by assessing its similarity with watermark slices from other clients with the same embedding frequency. The major contributions of this paper are as follows.

- To our knowledge, we propose the first robust model ownership protection framework for personalized federated learning. This framework enables private watermark embedding and model ownership verification for clients.

- By decoupling the watermark embedding process and adopting watermark slices, RobWE effectively addresses the watermark interference issue arising from model aggregation in FL. This strategy greatly enhances flexibility, allowing more clients to embed multiple watermarks.
- By employing the data distribution characteristics of watermark slices from clients with identical embedding frequencies, we design a tamper-resistant watermark detection mechanism, which can accurately detect malicious clients.
- We comprehensively evaluate RobWE and demonstrate that RobWE significantly outperforms the state-of-the-art watermark embedding schemes in FL regarding fidelity, reliability, and robustness.

2. Related Work

2.1. Watermarking in Centralized Learning

Watermarking is a technique designed to prevent models from being stolen and copied by others. By embedding watermarks into the model, the model owner is able to prove the attribution of the model. One way to achieve this is to change the parameters or the structure of the model. This involves schemes such as embedding bit strings in the loss function [32] or a particular activation layer [5], fine-tuning pre-trained models to embed identifiable fingerprints [2], adjusting the GAN-like structure for more covert watermark generation [33], adding a special task-agnostic barrier [38] and introducing a passport layer to prevent ambiguity attacks [8, 9]. Another way is to use trigger sets to train as a backdoor to the model. Lin *et al.* [21] generated trigger sets using a key from the authority to create a scrambling sequence that shuffles pixels and assigns original labels. Zhang *et al.* [37] introduced various methods to generate watermarking keys, which are then utilized in fine-tuning pre-trained models. Guo and Potkonjak [11] contributed a technique leveraging evolutionary algorithms to generate and optimize patterns for backdoor watermarking.

2.2. Watermarking in Federated Learning

To protect the intellectual property of models in FL, Tekgul *et al.* [30] treated the server as the model owner and embed the backdoor-based watermark in the aggregation phase. However, the server does not always take ownership of the model. Liu *et al.* [22] proposed embedding backdoor-based watermarks on the client side. Li *et al.* [17] proposed FedIPR to embed feature-based and backdoor-based watermarks on all clients. This scheme applies to the existing FL problem settings. However, when the number of clients increases, the watermark protection undergoes significant performance degradation. More importantly, the aforementioned schemes have not accounted for the need for intellectual property protection in PFL scenarios. Furthermore,

these schemes are susceptible to embedded watermarking attacks, such as model fine-tuning [32] and model pruning [5]. To thwart these attacks, some schemes [20, 28, 35] were proposed to trace the leaked malicious client back. Nevertheless, none of them can prevent malicious clients from tampering with the watermark during the watermark embedding phase, let alone the watermark conflicts during model aggregation.

3. Problem Statement

In this section, we first present tampering and adaptive tampering attacks during watermark embedding. Then, we formally define the watermark embedding problem in PFL.

3.1. Tampering Attack

In previous studies [35, 36], the server sends a shared watermark to clients, who can maintain ownership of the model by embedding this shared watermark. However, malicious clients can remove the shared watermark by embedding a tampered watermark, rendering it impossible to determine ownership of the leaked model. Suppose the original watermark is b_i , and the watermark tampering rate is f_t . Launching the tampering attack means flipping the number of bits in b_i by a proportion of f_t . Obviously, as f_t increases, the detection rate of the original watermark will gradually decrease and even drop to 0, thus achieving the purpose of model stealing.

3.2. Adaptive Tampering Attack

We further consider the evolved version of the tampering attack, where clients can collude to launch tampering attacks, referred to as adaptive tampering attacks. And we assume that honest clients are the majority. Here, we evaluate the effectiveness of the attack against FedIPR [17] and our proposed RobWE. In this experiment, we consider 20% and 40% of clients are malicious, who tamper with the watermark to be embedded during the training process, with each attack tampering with 10% bits of the watermark. We implement our scheme without defense to demonstrate the impact of adaptive tampering attacks. As shown in Fig. 1(a) and (b), as the ratio of malicious clients launching adaptive tampering attacks increases in FedIPR, the detection rate of tampered watermarks embedded by malicious clients becomes greater than that of the watermarks embedded by honest clients, resulting in the theft of model ownership during the embedding process. In comparison, as shown in Fig. 1(c) and (d), under RobWE, without taking any attack detection, malicious clients can only approach the watermark detection rate of honest clients and cannot completely dominate.

The reason is that RobWE adopts a watermark slice operation, which allows the server to assign different watermark slices to each client and embed them in different re-

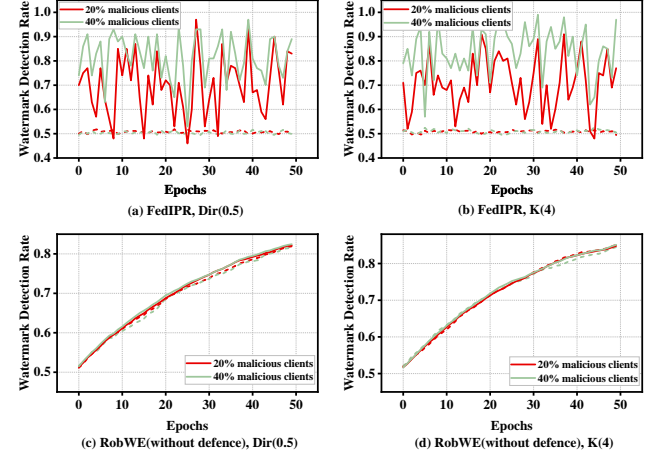


Figure 1. In the Non-IID settings (i.e., Dir(0.5) and K(4)), the watermark detection rates of malicious clients (solid line) and honest clients (dashed line) in FedIPR and RobWE (without defense).

gions. In this way, clients are unaware of the other watermark slices, preventing malicious clients from simply tampering with the watermark to remove it. In contrast, FedIPR embeds the client watermarks in the same region, resulting in malicious clients launching adaptive tampering attacks very easily. Moreover, watermarks embedded in the same region interfere with each other, which not only poses the capacity issue but also fails to satisfy the urgent demand of PFL for unique private ownership of models.

3.3. Problem Definition

Inspired by prior works [4, 32] and the above observations, we characterize the watermark embedding problem in PFL based on the following two tasks:

- **Main task** is to achieve the goal of PFL. Here, we adopt the idea of representation learning [1, 4, 40] to achieve model training. Formally, we consider a PFL setting consisting of a global common representation m_r , which is a function parameterized by $r \in \mathcal{R}$ learned by all clients, and client-specific heads m_{h_i} , which are functions parameterized by $h_i \in \mathcal{H}$ learned individually by each client i . Here, \mathcal{R} and \mathcal{H} are global common representation solution space and head solution space, respectively. Then, the global objective of PFL is formulated as:

$$\min_{r \in \mathcal{R}} \frac{1}{n} \sum_{i=1}^n \min_{h_i \in \mathcal{H}} f_i(h_i, r), \quad (1)$$

where $f_i(h_i, r)$ is an expected risk function. In this way, clients can collaboratively learn shared m_r using data from all clients while optimizing private m_{h_i} only using their own personal data.

- **Embedding task** is to achieve watermark embedding in PFL. Given a model m consisting of m_r and m_{h_i} , the em-

bedding task is to embed an l -bit vector $b \in \{0, 1\}^l$ into the parameters of one or more layers of the personalized model. Similar to prior works [17, 32], we introduce the regularization term to the learning objective of the main task and use the Hamming distance $H(b, \tilde{b})$ to verify the embedding effect of the watermark, where b is the target watermark to be embedded and \tilde{b} is the extracted watermark. After watermark embedding, each client's personalized model should include a private watermark that cannot be disrupted by other watermarks and resists the proposed tampering attack and other common watermarking attacks, thus distinguishing it from previous solutions.

4. Proposed Scheme

4.1. Overview of RobWE

The RobWE framework is shown in Fig. 2, and the workflow in each step is described as follows.

- **System Setup.** Each client i generates local watermarks, including a private watermark information Θ_i and a watermark slice information Ω_i obtained from the server.
- **Watermark Decoupled Embedding.** Clients embed watermark slices and private watermarks in the representation layer m_r and model head layer m_h , respectively.
- **Tampered Watermark Detection.** The server detects and rejects clients who attempt to embed tampered watermarks before each round of model aggregation.

4.2. System Setup

Each client i firstly obtains the initial global model m^0 from the server and generates its own private watermark information $\Theta = (b_i, \theta_i, E_i)$, where b_i is the watermark to be embedded into m_{h_i} , θ_i denotes the location of the watermark, and E_i denotes the embedding matrix. Notably, the size of E_i varies according to θ_i . For example, if client i sets $\theta_i = \{c_1, c_2\}$, this indicates that b_i is to be embedded into the first and second convolutional layers c_1 and c_2 . Then, b_i will be divided into $b_i^{c_1}$ and $b_i^{c_2}$ according to Eq. (2), where l is the length of b_i and the subscript j represents the index of each bit in b_i . The symbol $||$ denotes the number of parameters in the corresponding layer. Accordingly, client i generates embedding matrices $E_i = \{E_i^{c_1}, E_i^{c_2}\}$, where $E_i^{c_k}$ ($k \in \{1, 2\}$) is generated from the standard normal distribution $\mathcal{N}(0, 1)$ and the size is $|c_k| \times |b_i^{c_k}|$.

$$\begin{cases} b_i^{c_1} = \{b_{ij}\}_{j=1}^{j=\lfloor \frac{|c_1|}{|c_1|+|c_2|} \times l \rfloor} \\ b_i^{c_2} = \{b_{ij}\}_{j=\lfloor \frac{|c_1|}{|c_1|+|c_2|} \times l \rfloor+1}^{j=l}. \end{cases} \quad (2)$$

In addition, the server generates a common watermark b_S and divides it into various watermark slices b_{S_i} . The b_{S_i} is then sent privately to client i along with the embedding location ω_{S_i} and embedding matrix E_{S_i} , i.e., the watermark

Algorithm 1 Watermark Decoupled Embedding

Input: p : sampling rate; n : number of clients; T : total training rounds; Ω_i : watermark slice information; λ : learning rate; m^0 : the initial global model;

Output: Personalized models m_i with watermarks

- 1: Server sends Ω_i and m^0 to each client i
- 2: **for** $t = 1, 2, \dots, T$ **do**
- 3: Server samples a batch of clients \mathcal{C}^t of size pn
- 4: Server sends representation model m_r^t to clients
- 5: **for** client i in \mathcal{C}^t **do**
- 6: Client i initializes $m_{h_i}^t \leftarrow m_{h_i}^{t-1, \xi}$
- 7: **for** $\epsilon = 1$ to ξ **do**
- 8: $m_{h_i}^{t, \epsilon+1} \leftarrow \text{GRD}(L_{h_i}, m_{h_i}^{t, \epsilon}, \lambda)$
- 9: **end for**
- 10: $m_{r_i}^{t+1} \leftarrow \text{GRD}(L_{r_i}, m_{r_i}^{t, \xi}, \lambda)$
- 11: Client i sends updated $m_{r_i}^{t+1}$ to server
- 12: **end for**
- 13: **for** client i not in \mathcal{C}^t **do**
- 14: Set $m_{h_i}^{t+1, \xi} \leftarrow m_{h_i}^{t, \xi}$
- 15: **end for**
- 16: Server aggregates the new representation as $m_r^{t+1} = \frac{1}{pn} \sum_{i \in \mathcal{C}^t} m_{r_i}^{t+1}$
- 17: **end for**
- 18: **return** m_i consists of $m_{h_i}^{T, \xi}$ and m_r^T

slice information Ω_i equals $(b_{S_i}, \omega_{S_i}, E_{S_i})$. Since b_{S_i} will be embedded in the common part of the model, to avoid watermarking conflicts, ω_{S_i} requires not to overlap each other.

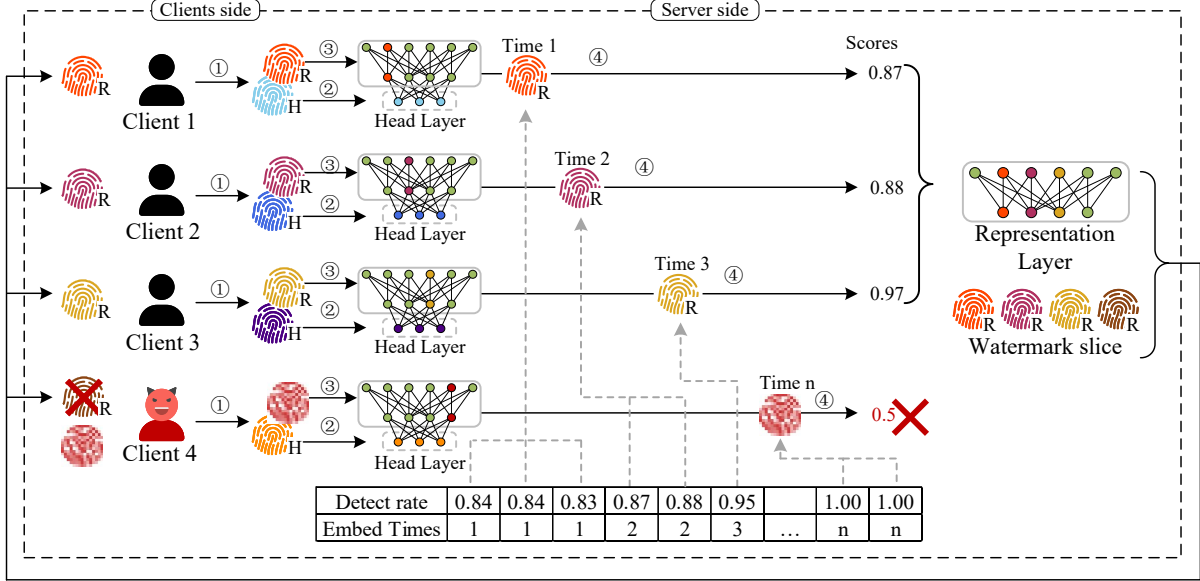
4.3. Watermark Decoupled Embedding

In this step, clients should complete the main and embedding tasks. The main idea of this step is to decouple the watermark embedding and model training. Specifically, model training involves head training and representation training, while model aggregation only occurs during representation training. Details of these operations are described below and summarized in Algorithm 1.

- **Head Training and Embedding.** In each round of model training, a certain percentage $p \in (0, 1]$ of clients are sampled to participate in the workflow. For each selected client i , it performs ξ times local update and watermark embedding only in the head layer of the model. Specifically, in the t training round, for $\epsilon = 1, 2, \dots, \xi$, client i adopts the embedding loss defined in Eq. (3) to update $m_{h_i}^{t, \epsilon}$, i.e., the head layer of model,

$$L_{h_i} = L_{\mathcal{D}_i}(m^{t, \epsilon}) + L_{\Theta_i}(m_{h_i}^{t, \epsilon}), \quad (3)$$

where $L_{\mathcal{D}_i}(m^{t, \epsilon})$ and $L_{\Theta_i}(m_{h_i}^{t, \epsilon})$ are the loss function of the main task and embedding task for embedding a private watermark in m_{h_i} . Followed by prior works [17, 32],



① Generates Local Watermarks ②Head training and embedding ③Representation Training and Embedding ④Tampered Watermark Detecting

Figure 2. An illustration of RobWE.

$L_{\Theta_i}(m_{h_i}^{t,\epsilon})$ can be defined as Eq. (4),

$$L_{\Theta_i}(m_{h_i}^{t,\epsilon}) = BCE(b_i, \tilde{b}_i) = BCE(E_i \times \overline{m_{h_i}^{t,\epsilon}}, b_i), \quad (4)$$

where $BCE(\cdot)$ is the binary cross entropy function and $m_{h_i}^{t,\epsilon}$ is the one-dimensional vector after flattening $m_{h_i}^{t,\epsilon}$. Formally, the head training and embedding can be expressed as Eq. (5),

$$m_{h_i}^{t,\epsilon+1} \leftarrow \text{GRD}(L_{h_i}, m_{h_i}^{t,\epsilon}, \lambda), \quad (5)$$

where $\text{GRD}(\cdot)$ represents a gradient updating method such as stochastic gradient descent (SGD) [19], and λ represents the learning rate.

- **Representation Training and Embedding.** After performing head training and embedding, the sampled clients perform representation training and embedding once only in $m_{r_i}^{t,\epsilon}$, i.e., the representation layer of the model. Specifically, the embedding loss for updating $m_{r_i}^{t,\epsilon}$ is denoted as Eq. (6),

$$L_{r_i} = L_{\mathcal{D}_i}(m^{t,\epsilon}) + L_{\Omega_i}(m_{r_i}^{t,\epsilon}), \quad (6)$$

where $L_{\Omega_i}(m_{r_i}^{t,\epsilon})$ is defined in Eq. (7), which represents the embedding loss caused by the inconsistency between the watermark slice extracted from the $m_{r_i}^{t,\epsilon}$ (i.e., \tilde{b}_{S_i}) and the target watermark slice (i.e., b_{S_i}).

$$\begin{aligned} L_{\Omega_i}(m_{r_i}^{t,\epsilon}) &= BCE(b_{S_i}, \tilde{b}_{S_i}) \\ &= BCE(E_{S_i} \times \overline{m_{r_i}^{t,\epsilon}(\omega_{S_i})}, b_{S_i}). \end{aligned} \quad (7)$$

Notably, the symbol $\overline{m_{r_i}^{t,\epsilon}(\omega_{S_i})}$ represents only the parameter at the ω_{S_i} position of $m_{r_i}^{t,\epsilon}$ that needs to be flattened since b_{S_i} is only embedded in certain regions of the

representation layer. Likewise, the representation training and embedding can be formalized as in Eq. (8).

$$m_{r_i}^{t+1} \leftarrow \text{GRD}(L_{r_i}, m_{r_i}^{t,\epsilon}, \lambda). \quad (8)$$

Once the model training and embedding described above are completed, each sampled client only sends $m_{r_i}^{t+1}$ to the server. If we ignore the presence of malicious clients in the FL scenario, the server can aggregate the representation layer models uploaded by the sampled clients according to Eq. (9), where \mathcal{C}^t contains indexes of the sampled client in the t round.

$$m_r^{t+1} = \frac{1}{pn} \sum_{i \in \mathcal{C}^t} m_{r_i}^{t+1}. \quad (9)$$

4.4. Tampered Watermark Detection

Due to the risk of malicious clients embedding tampered watermarks in FL scenarios, we designed a tampered watermark detection mechanism. As observed from some experiments, we find that the watermark detection rates of malicious clients implementing tampered watermark embedding, along with the watermark detection rates of honest clients embedding watermarks normally, each basically obeys a normal distribution. Some results of the experiments can be seen in Fig. 5. Unfortunately, client sampling results in varying embedding times of the watermark slice, and the watermark detection rate varies significantly between clients in the same round, making detection very difficult.

To solve the above issues, the server first records watermark slice detection rates and embedding times for each

round of the uploaded $m_{r_i}^{t+1}$. Then, to avoid the inability to directly compare watermark detection rates horizontally due to sampling, for each $m_{r_i}^{t+1}$, the server searches all watermark slice detection rate records with the same embedding times as $m_{r_i}^{t+1}$. Finally, based on the three-sigma rule commonly adopted in anomaly detection schemes [23, 25], we design the following decision rule to detect malicious clients.

1. During the early stages of training, when the server has not detected enough malicious clients (i.e., the number of detected malicious clients satisfies $num_m < \beta$), the watermark slice detection accuracy acc_i defined in Eq. (10) should satisfy Eq. (11).

$$acc_i = 1 - \frac{1}{|b_{S_i}|} H(b_{S_i}, \tilde{b}_{S_i}), \quad (10)$$

$$acc_i > \mu_n - Z_{C_n} \times \frac{\sigma_n}{\sqrt{num_n}}, \quad (11)$$

where μ_n and σ_n are the mean and standard deviation of the detection rate of the searched watermarked slice with the same embedding times as $m_{r_i}^{t+1}$, respectively. The number of searched watermarked slices is denoted as num_n , and Z_{C_n} is the critical value that can be determined by confidence level C_n . In practice, C_n can be determined on a practical basis. For example, if tolerance for malicious clients is high, C_n can be set larger so that most of the clients will not be considered malicious early in the training.

2. When the number of malicious clients detected by the server is sufficient to characterize malicious clients, i.e., $(num_m \geq \beta)$, acc_i should satisfy Eq. (12), which implies acc_i does not match the characterize of malicious clients.

$$acc_i > \mu_m + Z_{C_m} \times \frac{\sigma_m}{\sqrt{num_m}}, \quad (12)$$

where μ_m and σ_m are the mean and standard deviation of the acc_i of the detected malicious clients, respectively. And Z_{C_m} is the critical value that can be determined by confidence level C_m . The C_m represents the optimism about accepting honest clients. For example, setting C_m to a relatively small value can ensure that most clients meet the upper bound requirement for the distribution of watermark detection rate among malicious clients, provided we assume that most clients are honest.

5. Experiments

5.1. Experimental Setup

- **Datasets.** We adopt CIFAR-10 [15], MNIST [16] and FMNIST [34] datasets, and utilize the Non-IID setup [18] for dataset division. Here, the notation $K(n)$ stands for

assigning n differently labeled data to each client, and $Dir(\beta)$ stands for constructing the data distribution for each client according to the Dirichlet distribution.

- **Baseline.** We compare RobWE with FedIPR [17], which allows clients to embed both backdoor-based and feature-based watermarks in the global model for ownership protection. To ensure a fair comparison, we solely use feature-based watermarks in FedIPR.
- **Models and Configurations.** We adopt convolutional neural network (CNN) [4] as the baseline model for PFL training, facilitating the verification of schemes' ability to embed watermarks on models with fewer parameters. We employ 100 clients using the SGD optimizer with a learning rate of 0.01 over 50 epochs. Local training consists of 11 epochs, divided into 10 for the head layer training and 1 for the representation layer training. The batch size is 10 with a sampling rate of 0.1.
- **Metrics.** We evaluate RobWE in the following aspects:
 1. **Fidelity.** We adopt the accuracy of the main task as the fidelity metric and investigate the relative variation in accuracy when adding the maximum watermarked bits, defined as Gap, compared to a model without any embedded watermarks. A smaller Gap indicates higher fidelity.
 2. **Reliability.** We utilize the watermark detection rate and the range of variation under embedding different sized watermarks to measure reliability.
 3. **Robustness.** We use watermark detection rate w to reflect robustness under pruning, fine-tuning, and tampering attacks. For tampering attacks, the tamper detection rate d_t , false positive rate d_f and the discrepancy between watermark detection rates of honest and malicious clients, denoted as Δ_{w_n, w_m} , are employed to gauge the defensive effectiveness.

5.2. Experimental Results

5.2.1 Fidelity Performance

We embed watermarks with various bits using RobWE and FedIPR under different Non-IID settings. Tab. 1 shows that RobWE has a higher model accuracy compared to FedIPR in most cases, with Gap values ranging from 0.14% to 8.85% much smaller than the range of Gap values for FedIPR. This indicates that RobWE is not only able to obtain personalized models with better accuracy, but also has very little negative impact on model accuracy as the number of watermark embedded bits increases. On the contrary, for FedIPR, the accuracy steadily decreases as the number of watermarked bits increases, with a Gap between 28.83% and 88.67%. The model accuracy in the worst scenario drops to 11.03%, a drop of 88.67% compared to the case without watermarking, making the model unadoptable.

DataSet	NonIID	RobWE (v.s. FedIPR)				
		0 bit	50 bits	100 bits	150 bits	Gap
CIFAR-10	Dir(0.1)	88.11 (26.63)	87.77 (15.09)	87.99 (12.88)	87.53 (14.40)	0.66% (45.93%)
	Dir(0.3)	75.70 (46.94)	74.89 (33.65)	73.76 (21.40)	73.63 (12.77)	2.72% (72.80%)
	Dir(0.5)	68.82 (68.28)	68.69 (29.01)	68.09 (11.74)	67.71 (9.98)	1.61% (85.38%)
	K(2)	87.48 (17.31)	86.62 (15.56)	86.18 (12.46)	86.63 (12.32)	0.96% (28.83%)
	K(4)	70.43 (62.07)	70.57 (19.22)	69.31 (17.04)	66.25 (13.24)	5.93% (78.67%)
	K(6)	64.31 (69.73)	62.13 (38.54)	61.19 (21.11)	58.61 (14.26)	8.85% (79.55%)
MNIST	Dir(0.1)	99.38 (95.80)	99.36 (81.13)	99.28 (50.23)	99.23 (22.98)	0.14% (76.01%)
	Dir(0.3)	98.44 (97.72)	98.35 (94.92)	98.30 (50.24)	98.30 (11.35)	0.14% (88.39%)
	Dir(0.5)	97.96 (98.21)	97.76 (92.75)	97.49 (76.56)	97.44 (56.83)	0.54% (42.13%)
	K(2)	99.37 (97.29)	99.31 (23.06)	99.20 (16.49)	98.54 (11.03)	0.84% (88.67%)
	K(4)	97.90 (97.11)	97.85 (95.62)	97.54 (60.46)	97.37 (16.03)	0.53% (83.49%)
	K(6)	88.64 (98.54)	88.12 (95.11)	87.15 (81.08)	87.00 (38.00)	1.84% (61.44%)
FMNIST	Dir(0.1)	96.89 (64.04)	96.80 (38.85)	96.70 (20.50)	96.74 (11.02)	0.15% (82.79%)
	Dir(0.3)	91.79 (84.91)	91.64 (80.74)	91.10 (66.89)	89.73 (39.12)	2.24% (53.93%)
	Dir(0.5)	90.94 (86.76)	90.92 (82.60)	90.13 (69.43)	89.92 (54.20)	1.12% (37.53%)
	K(2)	95.99 (80.07)	95.02 (62.47)	92.00 (65.59)	91.08 (51.93)	5.12% (35.14%)
	K(4)	92.60 (81.51)	92.44 (67.72)	92.21 (37.28)	92.05 (16.66)	0.59% (79.56%)
	K(6)	79.43 (85.75)	78.10 (82.42)	78.09 (70.17)	76.95 (24.30)	3.12% (71.66%)

Table 1. The model accuracies after embedding different bits of watermarks and the relative variation values (i.e., Gap) of the model accuracies when embedding the maximum watermarks compared to those when the watermarks are not embedded.

5.2.2 Reliability Performance

Following [17], we select 10 clients to participate in model watermark embedding without sampling operation. Each client embeds a private watermark of 50 bits, 100 bits and 150 bits under $Dir(0.5)$ and $K(4)$ Non-IID settings, respectively. After embedding, we extract the watermarks of all clients on each client’s model and calculate the watermark detection rate. As shown in Fig. 3, we use multiple heatmaps to show the detection rate of all clients’ watermarks detected on each client’s private model, with darker colors representing higher detection rates. The diagonal position represents the detection rate of the client’s own private watermark. The results show that the watermark detection rate of each client’s private watermark in RobWE is significantly greater than that of other clients (non-diagonal region), while the private watermark detection rate of each client in FedIPR is even worse than that of other clients’ watermarks since the client’s model is mixed with the watermarks of other clients. Additionally, the baseline model we used for embedding watermarks has only 128 channels. As shown in Tab. 2, RobWE also significantly outperforms FedIPR when the watermark occupancy is much larger than the maximum watermark occupancy threshold (10%, where FedIPR can guarantee a watermark detection rate of 1).

5.2.3 Robustness Performance

To illustrate robustness to common attacks on watermarking, we perform a pruning attack [27] and a fine-tuning at-

Bits	Occupancy Ratio	Range (RobWE vs. FedIPR)
50	39.06%	(0.98,1)/(0.58,0.78)
100	78.13%	(1,1)/(0.57,0.68)
150	117%	(0.99,1)/(0.49,0.66)

Table 2. The model channel occupancy ratio for different size of watermarks and the range of variation in the watermark detection rate under corresponding embedding scenarios.

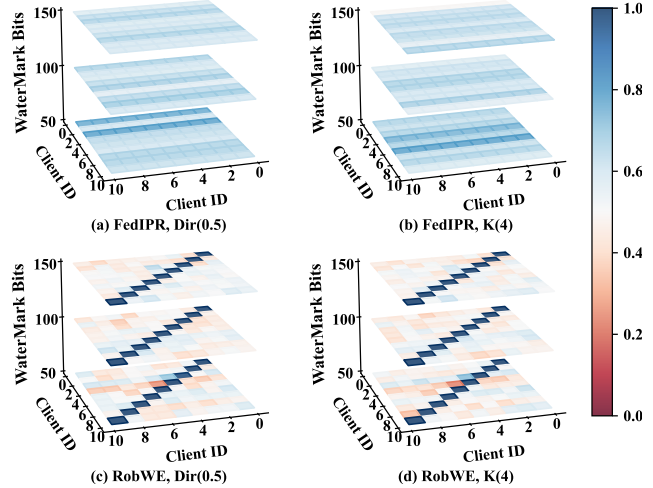


Figure 3. The watermark detection rate for other client watermarks on each client’ model (non-diagonal region) and the detection rate for own private watermarks (diagonal region).

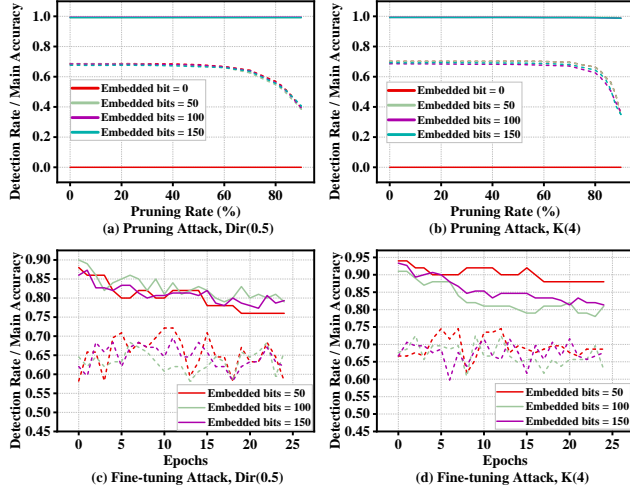


Figure 4. In the Non-IID setting, the model accuracy (dashed line) and watermark detection rates (solid line) of models with different embedded bits watermark after attacks.

tack [17] against private watermarks embedded in the head layer, respectively. As shown in Fig. 4(a) and (b), as the pruning rate increases, more and more model parameters are removed, and when the ratio reaches 70%, the accuracy of the model already starts to decrease, but the watermark detection rate remains stable at a high level. Therefore, RobWE is highly resistant to pruning attacks.

To implement fine-tuning attacks, honest clients first train 50 rounds and embed their private watermarks. Then, the attacker locally trains 25 rounds of fine-tuning based on these trained models. Fig. 4(c) and (d) show that although the watermark detection rate decreases during the model fine-tuning process, the overall rate remains above 0.75, which is still effective for ownership authentication.

Then, we perform the adaptive tampering attack against the representation layer of the model. The effect has been displayed in Fig. 1, where malicious clients' watermark detection rate is greater than or obfuscates honest clients' watermarks. We further increase the fraction of malicious clients f_m and the watermark tampering rate f_t . The larger the gap between the watermark detection rate of honest clients and the watermark detection rate of malicious clients Δ_{w_n, w_m} after applying defenses indicates greater resistance to tampering attacks. Tab. 3 shows that Δ_{w_n, w_m} is still significant even if the malicious client has only been tampered with a very small portion (i.e., 0.1). In fact, the smaller the f_t , the harder it is for the attacker to be detected. Under various settings, our method consistently maintains a malicious client detection rate of more than 0.9 and a maximum false positive rate of no more than 0.05.

Meanwhile, Fig. 5 shows that the watermark detection rates of malicious and honest customers basically satisfy the normal distribution. In fact, we chose C_n of 0.975 and C_m

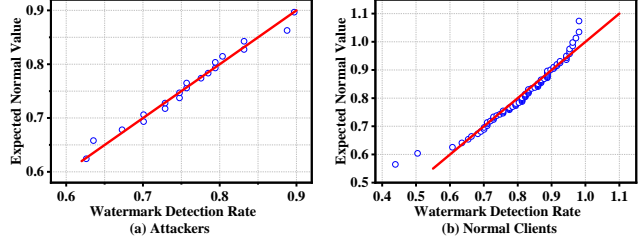


Figure 5. The Quantile-Quantile plot for assessing whether the watermark detection rate between normal clients and attackers obeys a normal distribution.

NonIID	(f_m, f_t)	w_n	w_m	d_t	d_f	Δ_{w_n, w_m}
Dir(0.5)	(0.2, 0.1)	95.42	86.65	0.95	0.01	8.77
	(0.2, 0.3)	96.19	87.33	1.0	0	8.86
	(0.4, 0.1)	97.45	79.44	0.95	0	18.01
	(0.4, 0.3)	96.34	79.97	0.9	0	16.37
K(4)	(0.2, 0.1)	95.43	84.29	1.0	0.05	11.14
	(0.2, 0.3)	95.43	86.24	1.0	0.04	9.19
	(0.4, 0.1)	95.93	79.11	0.975	0	16.82
	(0.4, 0.3)	94.61	80.03	0.925	0	14.58

Table 3. The detection performance (d_t) of RobWE on malicious clients under various proportions of malicious clients (f_m) and tampering rates (f_t).

of 0.5 for detection. The former is a direct adoption of the 3σ detection interval, while the latter adopts neutrality to accept honest clients. In practice, this can be adjusted according to the actual situation, while not being limited to the requirement of strictly meeting the normal distribution.

6. Conclusion

This paper presents a robust watermark embedding scheme, named RobWE, to protect the ownership of personalized models in PFL. RobWE decouples the watermark embedding procedure into head layer embedding and representation layer embedding, allowing clients to embed individual private watermarks independently of model aggregation. Furthermore, we propose a watermark slice embedding method for embedding non-overlapping watermark slices in the shared representation layer to facilitate contribution proof by each client. Additionally, for the proposed tampering attack, we couple with a dedicated detection scheme aimed at improving robustness. Through a series of experiments, we comprehensively evaluate the performance of RobWE, and the results show that our scheme successfully safeguards personalized model ownership in PFL. In the future, we will consider designing tamper-resistant watermark embedding schemes under both an untrusted server and malicious clients. We also plan to design a model leakage tracing mechanism for PFL.

References

[1] Yue Bai, Dipu Manandhar, Zhaowen Wang, John P. Collomosse, and Yun Fu. Layout representation learning with spatial and structural hierarchies. In *AAAI*, pages 206–214, 2023. 3

[2] Huili Chen, Bita Darvish Rouhani, Cheng Fu, Jishen Zhao, and Farinaz Koushanfar. DeepMarks: a secure fingerprinting framework for digital rights management of deep learning models. In *ICMR*, pages 105–113, 2019. 2

[3] Yiqiang Chen, Wang Lu, Xin Qin, Jindong Wang, and Xing Xie. MetaFed: Federated learning among federations with cyclic knowledge distillation for personalized healthcare. *IEEE Transactions on Neural Networks and Learning Systems*, pages 1–12, 2023. 1

[4] Liam Collins, Hamed Hassani, Aryan Mokhtari, and Sanjay Shakkottai. Exploiting shared representations for personalized federated learning. In *ICML*, pages 2089–2099, 2021. 3, 6

[5] Bita Darvish Rouhani, Huili Chen, and Farinaz Koushanfar. DeepSigns: an end-to-end watermarking framework for ownership protection of deep neural networks. In *ASPLOS*, pages 485–497, 2019. 2, 3

[6] Kate Donahue and Jon M. Kleinberg. Model-sharing games: Analyzing federated learning under voluntary participation. In *AAAI*, pages 5303–5311, 2021. 1

[7] Alireza Fallah, Aryan Mokhtari, and Asuman Ozdaglar. Personalized federated learning with theoretical guarantees: a model-agnostic meta-learning approach. In *NeurIPS*, pages 3557–3568, 2020. 1

[8] Lixin Fan, Kam Woh Ng, and Chee Seng Chan. Rethinking deep neural network ownership verification: embedding passports to defeat ambiguity attacks. In *NeurIPS*, 2019. 2

[9] Lixin Fan, Kam Woh Ng, Chee Seng Chan, and Qiang Yang. DeepIP: deep neural network intellectual property protection with passports. *IEEE Transactions on Pattern Analysis and Machine Intelligence*, pages 1–1, 2021. 2

[10] Avishek Ghosh, Jichan Chung, Dong Yin, and Kannan Ramchandran. An efficient framework for clustered federated learning. pages 19586–19597, 2020. 1

[11] Jia Guo and Miodrag Potkonjak. Evolutionary trigger set generation for dnn black-box watermarking. 2019. 2

[12] Xuanli He, Qiongkai Xu, Yi Zeng, Lingjuan Lyu, Fangzhao Wu, Jiwei Li, and Ruoxi Jia. Cater: intellectual property protection on text generation apis via conditional watermarks. In *NeurIPS*, pages 5431–5445, 2022. 1

[13] Skylar Kolisko and Carolyn Jane Anderson. Exploring social biases of large language models in a college artificial intelligence course. In *AAAI*, pages 15825–15833, 2023. 1

[14] Kalpesh Krishna, Gaurav Singh Tomar, Ankur P. Parikh, Nicolas Papernot, and Mohit Iyyer. Thieves on sesame street! model extraction of BERT-based APIs. In *ICLR*, 2020. 1

[15] Alex Krizhevsky, Geoffrey Hinton, et al. Learning multiple layers of features from tiny images. 2009. 6

[16] Yann LeCun, Léon Bottou, Yoshua Bengio, and Patrick Haffner. Gradient-based learning applied to document recognition. *Proceedings of the IEEE*, 86(11):2278–2324, 1998. 6

[17] Bowen Li, Lixin Fan, Hanlin Gu, Jie Li, and Qiang Yang. FedIPR: ownership verification for federated deep neural network models. *IEEE Transactions on Pattern Analysis and Machine Intelligence*, pages 1–16, 2022. 1, 2, 3, 4, 6, 7, 8

[18] Qinbin Li, Yiqun Diao, Quan Chen, and Bingsheng He. Federated learning on Non-IID data silos: an experimental study. In *ICDE*, pages 965–978, 2022. 6

[19] Weiyu Li, Zhaoxian Wu, Tianyi Chen, Liping Li, and Qing Ling. Communication-censored distributed stochastic gradient descent. *IEEE Transactions on Neural Networks and Learning Systems*, 33(11):6831–6843, 2022. 5

[20] Junchuan Liang and Rong Wang. FedCIP: federated client intellectual property protection with traitor tracking. *CoRR*, abs/2306.01356, 2023. 3

[21] Huanjie Lin, Shuyuan Shen, and Haojie Lyu. Protecting IP of deep neural networks with watermarking using logistic disorder generation trigger sets. *Multimedia Tools and Applications*, 2023. 2

[22] Xiyao Liu, Shuo Shao, Yue Yang, Kangming Wu, Wenyuan Yang, and Hui Fang. Secure federated learning model verification: a client-side backdoor triggered watermarking scheme. In *SMC*, pages 2414–2419, 2021. 1, 2

[23] Xiaofeng Liu, Site Li, Yubin Ge, Pengyi Ye, Jane You, and Jun Lu. Ordinal unsupervised domain adaptation with recursively conditional gaussian imposed variational disentanglement. *IEEE Transactions on Pattern Analysis and Machine Intelligence*, pages 1–14, 2022. 6

[24] Brendan McMahan, Eider Moore, Daniel Ramage, Seth Hampson, and Blaise Aguera y Arcas. Communication-efficient learning of deep networks from decentralized data. 2017. 1

[25] David Ohana, Bruno Wassermann, Nicolas Dupuis, Elliot Kolodner, Eran Raichstein, and Michal Malka. Hybrid anomaly detection and prioritization for network logs at cloud scale. In *EuroSys*, page 236–250, 2022. 6

[26] Felix Sattler, Klaus-Robert Müller, and Wojciech Samek. Clustered federated learning: Model-agnostic distributed multitask optimization under privacy constraints. *IEEE Transactions on Neural Networks and Learning Systems*, 32(8):3710–3722, 2021. 1

[27] Abigail See, Minh-Thang Luong, and Christopher D Manning. Compression of neural machine translation models via pruning. 2016. 7

[28] Shuo Shao, Wenyuan Yang, Hanlin Gu, Jian Lou, Zhan Qin, Lixin Fan, Qiang Yang, and Kui Ren. FedTracker: furnishing ownership verification and traceability for federated learning model. *CoRR*, abs/2211.07160, 2022. 3

[29] Yun Shen, Xinlei He, Yufei Han, and Yang Zhang. Model stealing attacks against inductive graph neural networks. In *S&P*, pages 1175–1192, 2022. 1

[30] Buse G. A. Tekgul, Yuxi Xia, Samuel Marchal, and N. Asokan. Waffle: watermarking in federated learning. In *SRDS*, pages 310–320, 2021. 1, 2

[31] Florian Tramèr, Fan Zhang, Ari Juels, Michael K. Reiter, and Thomas Ristenpart. Stealing machine learning models via prediction APIs. In *USENIX Security*, pages 601–618, 2016. 1

- [32] Yusuke Uchida, Yuki Nagai, Shigeyuki Sakazawa, and Shin’ichi Satoh. Embedding watermarks into deep neural networks. In *ICMR*, pages 269–277, 2017. [2](#), [3](#), [4](#)
- [33] Tianhao Wang and Florian Kerschbaum. RIGA: covert and robust white-box watermarking of deep neural networks. In *WWW*, pages 993–1004, 2021. [2](#)
- [34] Han Xiao, Kashif Rasul, and Roland Vollgraf. Fashion-mnist: a novel image dataset for benchmarking machine learning algorithms, 2017. [6](#)
- [35] Wenyuan Yang, Yuguo Yin, Gongxi Zhu, Hanlin Gu, Lixin Fan, Xiaochun Cao, and Qiang Yang. FedZKP: Federated model ownership verification with zero-knowledge proof. *ArXiv*, abs/2305.04507, 2023. [2](#), [3](#)
- [36] Wenyuan Yang, Gongxi Zhu, Yuguo Yin, Hanlin Gu, Lixin Fan, Qiang Yang, and Xiaochun Cao. FedSOV: federated model secure ownership verification with unforgeable signature. *arXiv:2305.06085*, 2023. [3](#)
- [37] Jialong Zhang, Zhongshu Gu, Jiyong Jang, Hui Wu, Marc Ph. Stoecklin, Heqing Huang, and Ian Molloy. Protecting intellectual property of deep neural networks with watermarking. In *ASIACCS*, pages 159–172, 2018. [2](#)
- [38] Jie Zhang, Dongdong Chen, Jing Liao, Weiming Zhang, Huamin Feng, Gang Hua, and Nenghai Yu. Deep model intellectual property protection via deep watermarking. *IEEE Transactions on Pattern Analysis and Machine Intelligence*, 44(8):4005–4020, 2022. [2](#)
- [39] Yuheng Zhang, Ruoxi Jia, Hengzhi Pei, Wenxiao Wang, Bo Li, and Dawn Song. The secret revealer: Generative model-inversion attacks against deep neural networks. In *CVPR*, pages 250–258, 2020. [1](#)
- [40] Chen Zhao, Le Wu, Pengyang Shao, Kun Zhang, Richang Hong, and Meng Wang. Fair representation learning for recommendation: A mutual information perspective. In *AAAI*, pages 4911–4919. AAAI Press, 2023. [3](#)
- [41] Yue Zhao, Ishan Misra, Philipp Krähenbühl, and Rohit Girdhar. Learning video representations from large language models. In *CVPR*, pages 6586–6597, 2023. [1](#)